Effect of eccentric moments on seismic ratcheting of single-degree-of-freedom structures

K.Z. Saif, C.-L. Lee, G.A. MacRae & T.Z. Yeow

Department of Civil Engineering, University of Canterbury, Christchurch.

2017 NZSEE Conference

ABSTRACT: This study describes the background and provides validation of new provisions included in the 2016 amendment to NZS1170.5 to address ratcheting due to the presence of static eccentric moments. The validation was done by performing nonlinear time history analysis using a fibre model of a bridge column with a cracked section period of 1.0 s subjected to the FEMA P695 far-field ground motion suite. Peak and residual displacements were used as indicators of the degree of ratcheting. The effects of member axial loads and design force reduction factors on ratcheting were also investigated. It was found that the peak displacement demands increase with an increasing eccentric moment. The increase in displacement when the ratio of effective lateral strengths in the back-and-forth directions considering the presence of eccentric moment is 1.15 or less is lower than 10% compared to when equal lateral strengths were provided. Based on these findings, the ratcheting effect can be neglected for cases with low eccentric moments. When the effective strength ratio is increased to 1.86 and the eccentric moment applied is equal to 30% of the yield moment capacity, the peak displacements increased by more than 65% and residual displacements may also become close to the peak displacements. Design curves for estimating the displacement demands for different eccentric moments are provided.

1 INTRODUCTION

During earthquake shaking some structures tend to deform and yield more in one direction than in the other. This phenomenon, termed "ratcheting", can be caused by:

Ground motion effect, where the earthquake can excite the structure in one direction more than the other,

Dynamic stability effect, where the structures with negative dynamic stability (MacRae, 1994, Yeow et al., 2013), due to effects such as P-delta, bar fracture, and buckling, has a tendency to deform predominantly in the direction of first yielding or damage,

Structural form effect, where the structure has unbalanced strengths or stiffness's in the forward and reverse directions, and

Eccentric loading effect, which induces eccentric moments at the base of structures that changes the effective lateral strength of the structure and makes it yield more easily in the direction of eccentricity.

There are several known examples of ratcheting due to eccentric gravity loadings. One example is C-bent bridge columns, which are columns that support the bridge deck through cantilevered beams on one side only. They are usually used where the bridge column had to be offset due to space restrictions, such as allowing room for a right-turning lane as shown in Figure 1**Error! Reference source not found.**(a). Analytical and experimental studies on the seismic performance of C-bent columns was conducted by Kawashima et al. (2010), who showed that the column tended to deform predominantly in the direction of the eccentric moment. Damage was also observed in the compression face of the column in the direction of eccentric loading. Another example of this was the

Hotel Grand Chancellor building, which had a cantilevered eastern bay to make room for a walkway as shown on the right of Figure 1**Error! Reference source not found.**(b). Due to this, the building ratcheted 1.3m in the direction of the cantilevered bays during the 2011 February Canterbury earthquake (Royal Commission, 2011).

(a) C-bent column (courtesy of Yeow)

(b) Grand Chancellor Hotel (Royal Commission Report, 2011)

Figure 1: Examples of eccentric loaded structures

Previous studies (Kawashima et al., 1998; Yeow et al., 2013) explained ways of mitigating the ratcheting effect by increasing the strength in one direction to balance the eccentric moment effect. However, published studies to assess the increase in displacement if mitigation effects are not available. Such methods to estimate the increase in displacements would be useful as engineers usually perform modal or pushover structural analyses which are incapable of capturing ratcheting effects as it is an inelastic dynamics issue (Royal Commission, 2011).

The 2016 NZS1170.5 (2016) standard provides new provisions to account for ratcheting. While these provisions provide an index to indicate the tendency and quantify the effect of ratcheting due to structural form and eccentric loading index, there is a need to validate these provisions.

This paper seeks to address this need by finding answers to the following questions:

1. What is the effect of the eccentric moment on peak and residual displacements?
2. Are the new ratcheting provisions adequate?
3. How can peak and residual displacements be estimated when ratcheting caused purely by eccentric moments?

2 MECHANICS AND PROVISIONS TO ADDRESS SEISMIC BUILDING RATCHETING

2.1 Mechanics of ratcheting due to eccentric moments

Kawashima et al. (1998) and Yeow et al. (2013) summarised the dynamic stability concepts outlined by examining the ratcheting response of C-bent columns. They theorized that the "baseline" of the hysteresis loop shifts away from the zero-moment position by the size of the induced eccentric moment, M_E, as shown in **Error! Reference source not found.**. This in turn causes the relative strength in the "reverse" direction to decrease by M_E, while the relative strength in the "forward" direction increases by M_E. If the column had symmetric reinforcing, M_E would cause the effective strength in the reverse direction to be lower than that in the forward direction. This would cause yielding to predominantly occur in the reverse direction, which leads to ratcheting effects.

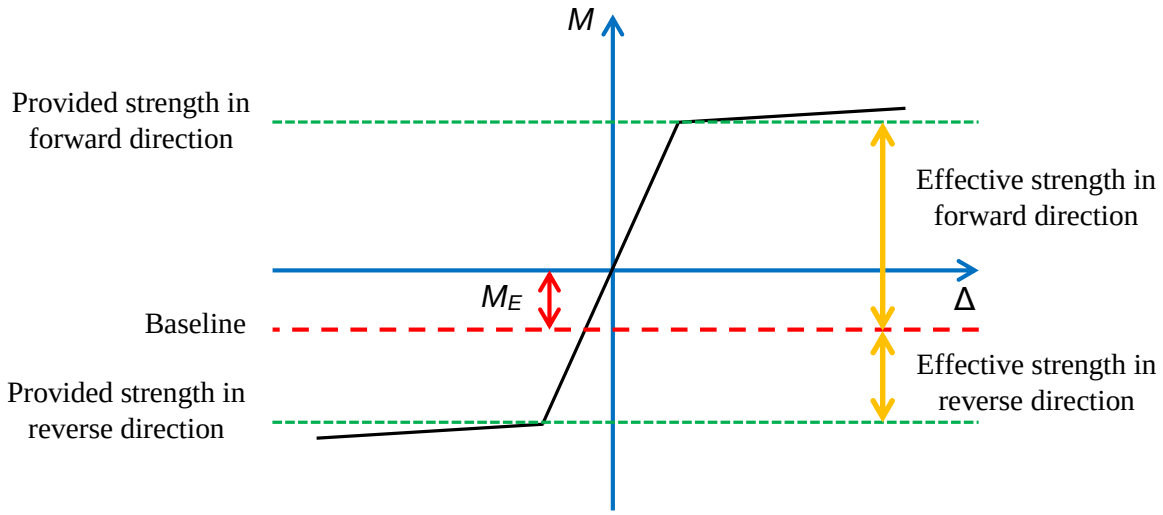

Figure 2: Ratcheting index terms

2.2 NZS1170.5 new provisions

Clause 4.5.3 in NZS1170.5 (2016) provides a methodology to calculate a ratcheting index, $r_{i,}$ which indicates the tendency for ratcheting and is shown in Equation 1. Here, r_1 accounts for the ratio of the column's effective lateral strengths in the back-and-forth directions caused by either eccentric moments and/or unbalanced strength and can be calculated by Equation 2; where the forward direction is defined as the direction of greater strength. r_2 accounts for any lateral strength difference in the opposite directions which balances out a portion of the eccentric gravity moment, and can be calculated by Equation 3.

$$r_i = r_1 + r_2 \tag{1}$$

$$r_1 = \frac{\text{Lateral strength in forward direction, } S_f}{\text{Lateral strength in reverse direction, } S_r} \tag{2}$$

$$r_2 = \frac{\text{Change in strength in forward direction, } S_g}{\text{Lateral strength in reverse direction, } S_r} \tag{3}$$

According to Clause 4.5.3 in NZS1170.5 (2016), the displacement demands will increase if r_i is larger than 1.0. Clause 7.3.1.2 states that the ratcheting effect is not considered to be significant and may be ignored if r_i is less than 1.15. If $1.15 < r_i < 1.5$ and the building's response was obtained without considering the eccentric loading, then peak displacements obtained should be increased by $0.75(r_i - 1)$ times the peak displacement. When the index r_i is greater than 1.5 the use of time-history analysis is required. The potential effect of force reduction factor, R, or the hysteresis loop shape is not considered in neither Clause 4.5.3 nor 7.3.1.2.

3 METHODOLOGY

The column adopted for this case study was based on a reinforced concrete bridge column with a scale of 2/5 used by Chang et al., (2004). This column has a height of 3.25 m with a cross section of 750 mm x 600 mm, as shown in **Error! Reference source not found.**. An axial force P and an eccentric moment M_E were applied at the top of the column.

The column was modelled as a fibre section using OpenSees (MacKenna et al., 2016). The unconfined concrete and streel fibre strengths were assumed to be 30 MPa and 300 MPa, respectively. The Concrete04 material, which is based on a uniaxial Popovics (1973) concrete material object, was used to model the concrete. The confined concrete area was assumed to be the rectangular area enclosed by the centroids of each individual longitudinal reinforcing bar, while the concrete in the cover area was

assumed to be unconfined. Steel02 material, which is based on a uniaxial Giuffre-Menegotto-Pinto (1973) steel material object, was used to model longitudinal reinforcement. The natural period, *T*, based on cracked section properties was kept constant at 1.0s.

Dynamic inelastic time history analyses were performed. The damping was modelled using 5% initial stiffness proportional Rayleigh damping in both modes. Nonlinear beam-column elements were used to model the nonlinear behaviour of the structural elements. P-delta effects were considered using the P-delta geometric transformation.

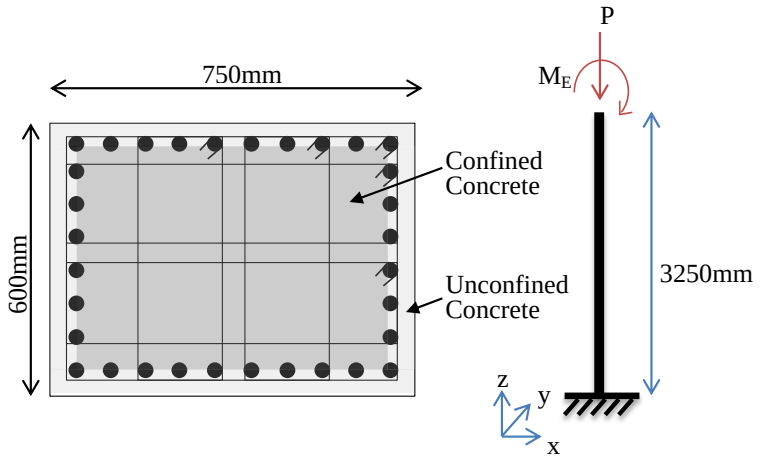

Figure 3: Cantilevered column model

The analysis framework adopted is shown in **Error! Reference source not found.**. The values of axial load ratio, which is *P* normalized by the axial load capacity, $A_g f'_c$, where A_g is the gross cross sectional area of the column and f'_c is the unconfined concrete strength, considered were 0.0, 0.1, and 0.2. The values of design force reduction factor, *R* (k_μ/S_p factor from Clause 5.2.1.1 in NZS1170.5), considered were 1, 2, 4 or 6. The eccentric moment ratio, α, is defined as the eccentric moment, M_E, normalized by the column's first yield moment, M_y, as shown in Equation 4, and was varied from 0.0 to 0.30 with a step size of 0.1.

$$\alpha = \frac{M_E}{M_y} \tag{4}$$

The far field records suggested in Appendix A of FEMA P695 (FEMA, 2009) were used. There are 22 ground motion records in total. The analysis was perform twice to eliminate directionality effects of the ground motions; once with the record applied in the forward direction, and the again in the reverse direction. For the cases where $R = 1$, each record was scaled such that the column just reached the yielding point. To account for higher values of *R*, the record magnitude scale factor calculated for $R = 1.0$ was multiplied by the target value of *R*. The final results were normalised with respect to the peak displacement at zero eccentric moment.

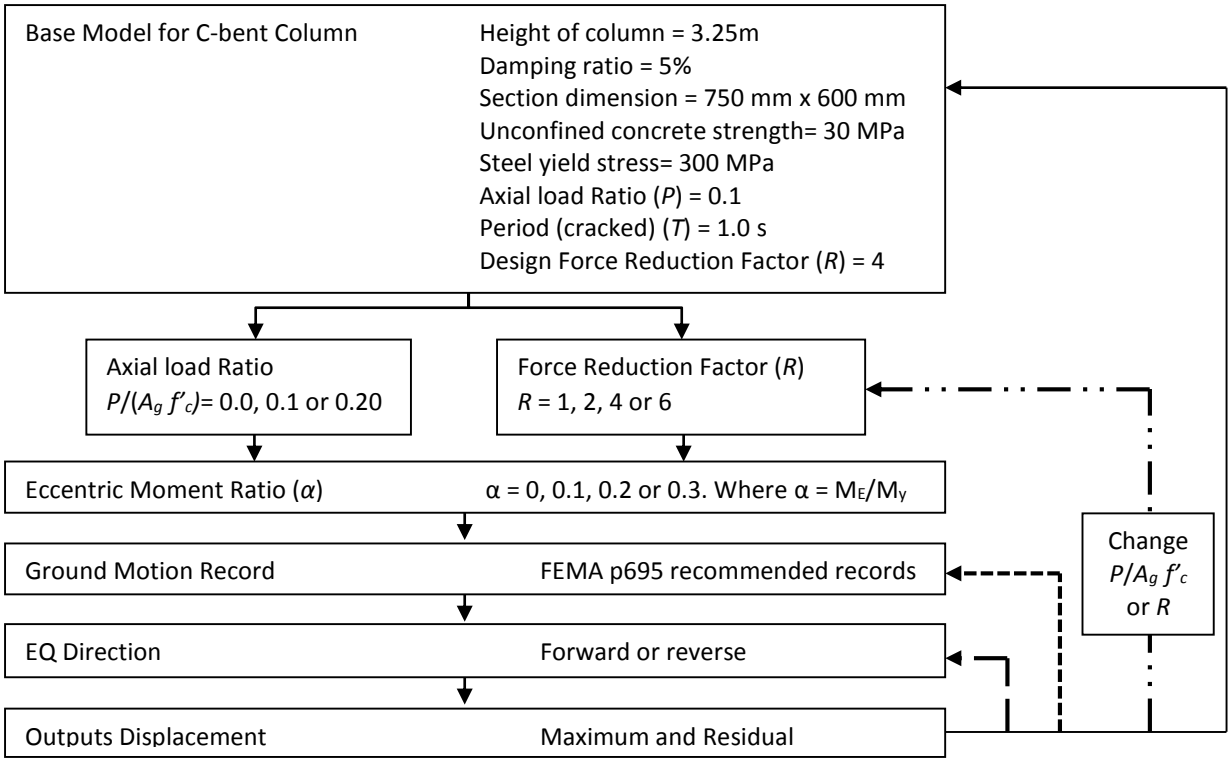

Figure 4: Analyses procedure

4 ECCENTRIC MOMENT EFFECT ON DISPLACEMENT DEMANDS

The influence of the eccentric moments on the column's response was defined by two parameters; peak displacement ratio (PDR) and residual displacement ratio (RDR). PDR and RDR are defined by Equations (5) and (6), respectively. Both PDR and RDR were calculated for each individual record and the average from all records is shown in **Error! Reference source not found.** and **Error! Reference source not found.**.

$$\text{PDR} = \frac{\text{Average peak displacement at } \alpha}{\text{Average peak displacement at } \alpha = 0} \tag{5}$$

$$\text{RDR} = \frac{\text{Average residual displacement at } \alpha}{\text{Average peak displacement at } \alpha = 0} \tag{6}$$

Error! Reference source not found. shows that displacements increase with increasing eccentric moment ratio, α. PDR is higher for a higher force reduction factor. This is because a weaker column would deform earlier, and therefore is more susceptible to eccentric loading effects. On the contrary, RDR is smaller for a high reduction factor, R. However, it should be noted that this does not mean that stronger buildings would have greater residual displacements. For example, if the yield moment capacity for R = 1 is 100 kNm, then M_E would be 5 kNm for α = 0.05. If the same size of M_E was applied to a column with R = 6 (16.7 kNm), α would therefore be 0.3. The corresponding average residual displacement ratios for these two cases would be 0.06 and 0.2, respectively. This demonstrates that residual displacements would likely increase with R as expected. As can be seen from **Error! Reference source not found.** when α = 0.3, the peak displacement could increase up to 60% for R = 6 and up to 35% for R = 1. These ratios show the importance of including ratcheting effect in design.

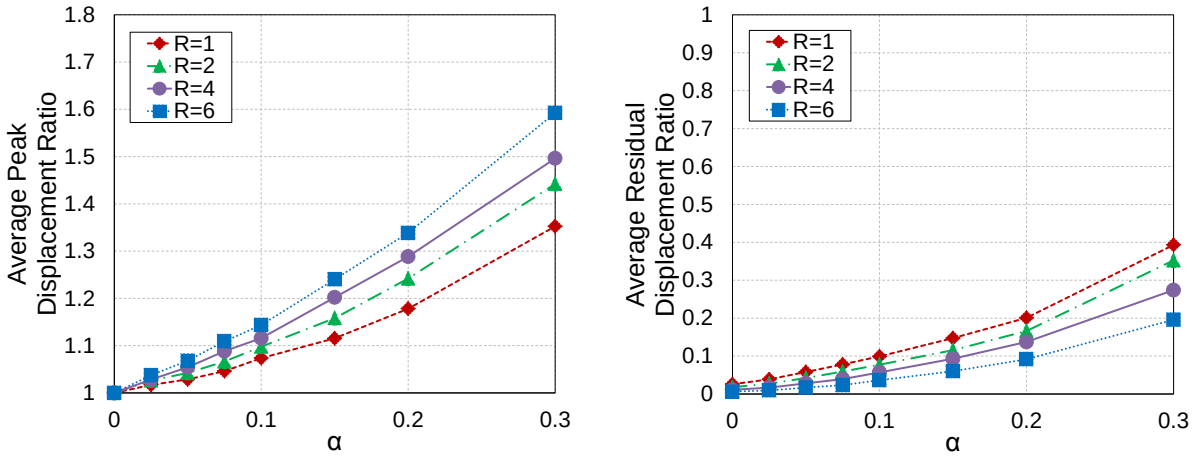

(a) Average peak displacement ratio

(b) Average residual displacement ratio

Figure 5: Effect of eccentric moments on displacement response with change in R (T=1s & P/A_gF_c=0.1)

Error! Reference source not found. shows the effect of the eccentric moment on displacements for different axial load ratios. As can be seen, the displacement demands increase with the increasing eccentric moment. The amount of increment decreases with the axial force. It is because the axial force enhances the re-centring capability of the column, resulting in reduced peak and residual displacements. An example of this is shown in **Error! Reference source not found.**, where the column subjected to $P/A_g\, f'_c$ = 0.2 exhibited re-centering characteristics while the $P/A_g\, f'_c$ = 0 case predominantly deformed in the positive direction. This effect would affect residual displacements more than peak displacements. **Error! Reference source not found.** also shows that the peak and residual displacement can increase by more than 65% and 90%, respectively, when P = 0.0 and α = 0.3.

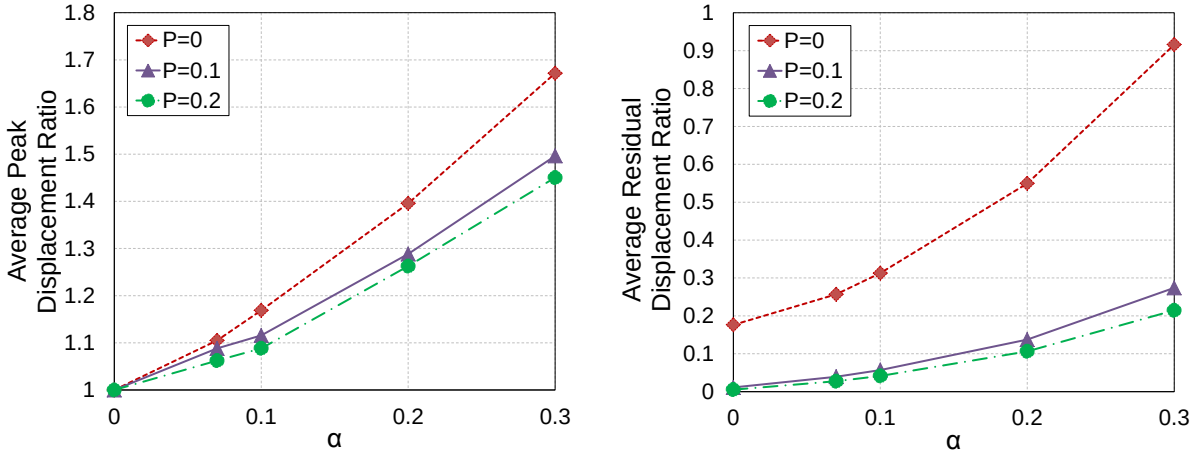

(a) Average peak displacement ratio

(b) Average residual displacement ratio

Figure 6: Effect of eccentric moments on displacement response with change in $P/A_g\, f'_c$ (T=1s & R=4)

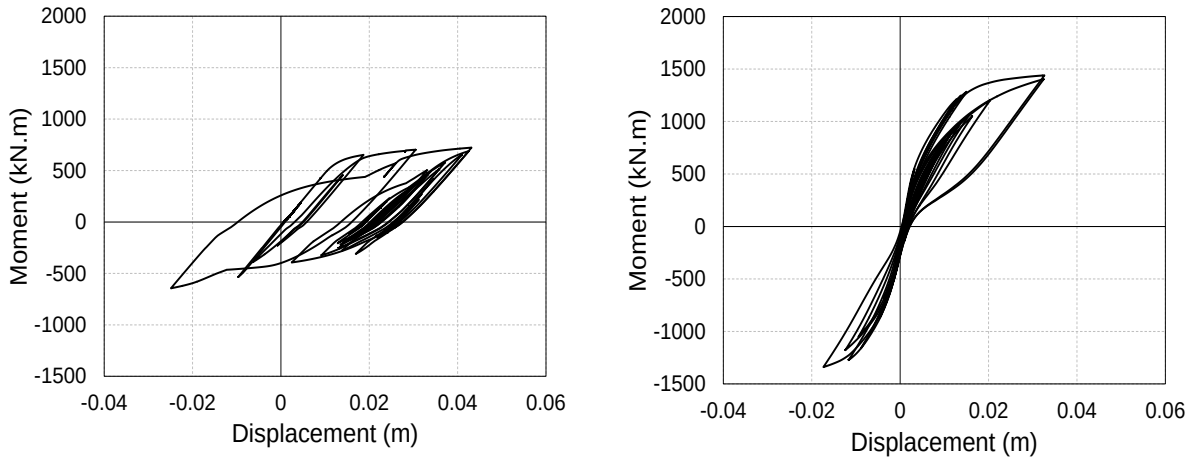

(a) Hysteresis loop for $P/A_g f'_c = 0$ (b) Hysteresis loop for $P/A_g f'_c = 0.2$

Figure 7: Effect of axial loading on hysteretic recentering characteristics (T = 1s, α = 0.2 & R = 4)

5 DISPLACEMENT ESTIMATION

Error! Reference source not found. and **Error! Reference source not found.** can be useful to estimate the peak and residual displacements for columns modelled without considering moment eccentricity. For example, consider a column designed for $P = 0.1f'_cA_g$ and R = 4 that has an estimated peak displacement of 100 mm without considering moment eccentricity. If α = 0.2, the corresponding peak and residual displacement ratios are 1.3 and 0.15, respectively, according to **Error! Reference source not found.**. Therefore, the expected peak and residual displacement considering eccentricity will be 130 mm and 15 mm, respectively.

6 NZS1170.5 NEW PROVISION VALIDATION

Based on the wording of Clause 4.5.3 in the new NZS1170.5 (2016) provisions, $r_2 = 0$ as the eccentric moment was not balanced by any increase in lateral strengths; resulting in $r_i = r_1$. The effective moment capacity in the forward direction is equal to the yield moment capacity plus M_E, while the capacity in the reverse direction is equal to the yield moment capacity minus M_E. Therefore, r_1 can be calculated according to Equation (7).

$$r_i = \frac{1+\alpha}{1-\alpha} \tag{7}$$

According to Clause 4.5.3 in NZS1170.5 (2016), when r_i is larger than 1.0, the displacement demands will increase due to ratcheting. Based on Equation (7), this requires α to be larger than zero. This is consistent with findings from **Error! Reference source not found.** and **Error! Reference source not found.**, where the displacement demands increase if α is larger than zero.

Clause 4.5.3 in NZS 1170.5 (2016) states that for cases where r_i between 1.15 and 1.5, Clause 7.3.1.2 can be used to estimate the increase in displacement demands. α corresponding to r_i = 1.15 and 1.5 are 0.07 and 0.2, respectively from Equation 7 assuming P = 0.0 and R = 6.0. The displacement would have to be increased by $0.75(r_i - 1)$, which is 11% and 38%, respectively. The corresponding values from Figures 5 and 6 are slightly lower at 10% and 35%, respectively. They are also generally lower for other values within this range. This indicates that Clause 7.3.1.2 provides conservative estimates for the range of parameters considered. The level of conservatism increases with greater axial force ratio and lower force reduction factor.

Clause 4.5.3 in NZS 1170.5 (2016) also states that if r_i is less than 1.15, the ratcheting effect is unlikely to be significant and can be neglected. Based on Equation (7), if r_i = 1.15, then α = 0.07. According to **Error! Reference source not found.** and **Error! Reference source not found.**, when α = 0.07, the increment in peak displacement ratios is less than 10% for any compressive axial force

ratio, T = 1s, and for R < 4. This is deemed reasonable, considering that variation in material strength, soil-structure interaction, and other factors may possibly result in such a change in building response on its own.

7 CONCLUSIONS

Dynamic inelastic time history analyses of a modeled reinforced concrete cantilever column with a period of 1.0s subjected to eccentric moments was performed. It was found that:

1. Eccentric moment caused peak and residual displacements to increase. For eccentric moment levels greater than 30% of the yield moment, peak and residual displacements increased by more than 65%, and 90%, respectively.

2. For the ratcheting index limit provided by NZS1170.5 where ratcheting does not need to be considered, r_i = 1.15, the eccentric moment ratio is 7%. At this, the median increase in response was less than 10% based on the analyses performed in this study. For 1.15 < r_i < 1.5, the displacement amplification factor proposed by new amendments to NZS1170.5 was found to provide reasonably conservative estimates.

In addition, graphs were developed to estimate the increase in peak and residual displacements due to the present of an eccentric moment. An example demonstrating its application was provided.

8 ACKNOWLEDGMENT

Sincere thanks are due to The Ministry of Foreign Affairs in New Zealand for awarding the first author the NZAID scholarship.

9 REFERENCES

Chang, Y.S., Li, Y.F. & Loh, C.H. (2004). Experimental study of seismic behaviors of as-built and carbon fiber reinforced plastics repaired reinforced concrete bridge columns. *Journal of Bridge Engineering*, ASCE 9(4), 391–402 doi:10.1061//ASCE/1084-0702/2004/9:4/391

Federal Emergency Management Agency (FEMA). (2009). Quantification of building seismic performance factors: FEMA P-695.

Kawashima K., MacRae G.A., Hoshikuma J. & Nagaya K. (1998). "Residual Displacement Response Spectrum", *ASCE Journal of Structural Engineering*, ASCE, pp. 523-530.

Kawashima, K., Seigi, N. & Watanabe, G. (2010). "Seismic performance of a bridge supported by C-bent columns," *Journal of Earthquake Engineering* 14(8), 1172–1220.

MacRae G.A. (1994). "P-Δ Effects on Single-Degree-of-Freedom Structures in Earthquakes", *Earthquake Spectra*, Vol. 10, No. 3, pp. 539-568.

McKenna, F., Fenves, G.L., Scott, M.H. & Jeremic, B. (2016). Open System for Earthquake Engineering Simulation (OpenSees). University of California, Berkeley.

Menegotto, M, Pinto, P.E. (1973). Method of analysis of cyclically loaded RC plane frames including changes in geometry and nonelastic behavior of elements under normal force and bending. Preliminary report IABSE, vol. 13, Zurich; p. 15–22.

Popovics, S. (1973). A numerical approach to the complete stress-strain curve of concrete. *Cement and Concrete Research*, 3(5), 583-599. doi:10.1016/0008-8846(73)90096-3

Royal Commission. (2011). Canterbury earthquakes Royal Commission interim report, Canterbury Earthquakes Royal Commissions Christchurch, N.Z.

Standards New Zealand. (2016). NZS1170.5:2004 Structural Design Actions Part 5 Earthquake actions New Zealand. Incorporating Amendment 1, 2016.

Yeow, T.Z., MacRae, G.A., Sadashiva, V.K. & Kawashima, K. (2013). Dynamic Stability and Design of C-Bent Columns. *Journal of Earthquake Engineering*, 17(5), 750-768. doi:10.1080/13632469.2013.771591